



Review

Cholesterol Regulation of Membrane Proteins Revealed by Two-Color Super-Resolution Imaging

Zixuan Yuan ^{1,2,3}  and Scott B. Hansen ^{1,2,*} ¹ Department of Molecular Medicine, Department of Neuroscience, UF Scripps, Jupiter, FL 33458, USA² Department of Neuroscience UF Scripps, Jupiter, FL 33458, USA³ Skaggs Graduate School of Chemical and Biological Sciences, The Scripps Research Institute, Jupiter, FL 33458, USA

* Correspondence: hansen.scott@ufl.edu

Abstract: Cholesterol and phosphatidyl inositol 4,5-bisphosphate (PIP₂) are hydrophobic molecules that regulate protein function in the plasma membrane of all cells. In this review, we discuss how changes in cholesterol concentration cause nanoscopic (<200 nm) movements of membrane proteins to regulate their function. Cholesterol is known to cluster many membrane proteins (often palmitoylated proteins) with long-chain saturated lipids. Although PIP₂ is better known for gating ion channels, in this review, we will discuss a second independent function as a regulator of nanoscopic protein movement that opposes cholesterol clustering. The understanding of the movement of proteins between nanoscopic lipid domains emerged largely through the recent advent of super-resolution imaging and the establishment of two-color techniques to label lipids separate from proteins. We discuss the labeling techniques for imaging, their strengths and weakness, and how they are used to reveal novel mechanisms for an ion channel, transporter, and enzyme function. Among the mechanisms, we describe substrate and ligand presentation and their ability to activate enzymes, gate channels, and transporters rapidly and potently. Finally, we define cholesterol-regulated proteins (CRP) and discuss the role of PIP₂ in opposing the regulation of cholesterol, as seen through super-resolution imaging.

Keywords: ion channel; transporter; PIP₂; lipid raft; nanoscopic; clustering

**Citation:** Yuan, Z.; Hansen, S.B.

Cholesterol Regulation of Membrane Proteins Revealed by Two-Color Super-Resolution Imaging.

Membranes **2023**, *13*, 250. <https://doi.org/10.3390/membranes13020250>

Academic Editor: Irina M. Le-Deygen

Received: 18 January 2023

Revised: 5 February 2023

Accepted: 7 February 2023

Published: 20 February 2023



Copyright: © 2023 by the authors. Licensee MDPI, Basel, Switzerland. This article is an open access article distributed under the terms and conditions of the Creative Commons Attribution (CC BY) license (<https://creativecommons.org/licenses/by/4.0/>).

1. Introduction

Elevated cholesterol is a key cellular component important to many metabolic and neurological diseases, including Alzheimer's, cardio-vasculature, diabetes, viral infections, and chronic inflammation [1–9]. A gap in understanding exists for how cholesterol affects many diverse biological functions. As a signaling molecule, cholesterol's major function is to cluster palmitoylated proteins (proteins containing a 155555 6-carbon lipid) with lipid rafts [10–13]. The lipid rafts are comprised of saturated ceramide-containing glycolipids (e.g., monosialotetrahexosylganglioside (GM1)) that bind palmitate with high affinity [11]. Clustered GM1 lipids are also referred to as GM1 clusters or GM1 domains.

Phosphatidylinositol 4,5 bisphosphate (PIP₂) is also a membrane-signaling lipid [14–18], and forms charged clusters separate from GM1-containing clusters [19–23] (Figure 1A). The distance between GM1 and PIP₂ clusters ranges from 42 nm in muscle cells [22] to ~200 nm in lung and kidney cells [7]. PIP₂ clusters are largely insensitive to cholesterol [19,20,22,23].

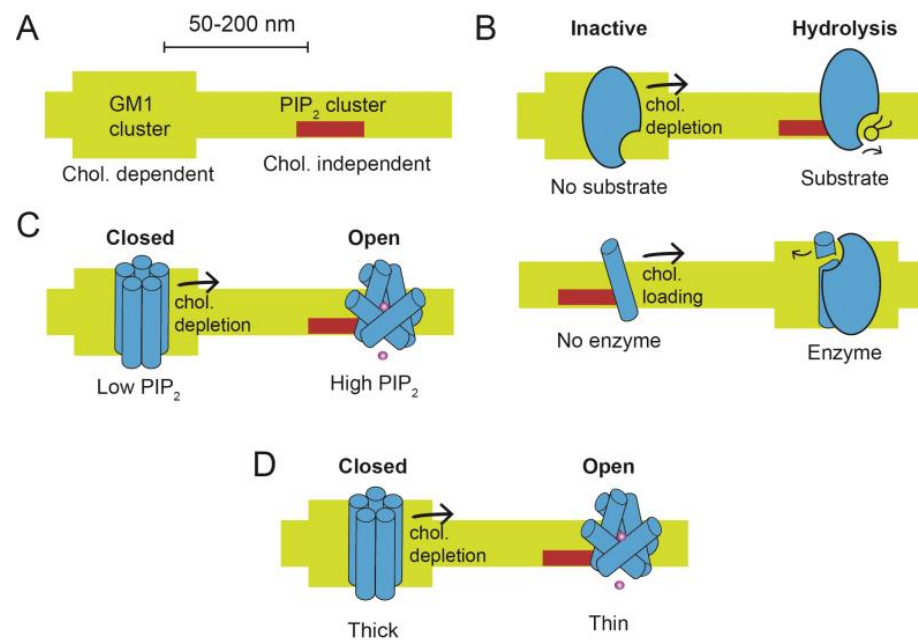


Figure 1. Cholesterol-regulated protein (CRP) activation by cholesterol depletion. (A) Two lipid domains are shown. On the left, saturated GM1 lipids are thick and form a cholesterol (chol.) dependent location. On the right, phosphatidylinositol 4,5 biphosphate (PIP₂) lipids are clustered and form cholesterol-independent locations. The two locations are separated by 50–200 nm in a cell membrane. (B–D) CRP proteins move in response to cholesterol depletion. In high cholesterol, proteins reside primarily in the GM1 location. In low cholesterol, they shift to or near the PIP₂ location. The shift to a new location produces at least three mechanisms of activation. In (B), CRP activation is shown by substrate presentation. (Top) An enzyme (blue shading) is inactive when sequestered in a GM1 lipid cluster, away from its substrate. When cholesterol is low, the GM1 domain is disrupted, and the enzyme moves (black arrow) to the PIP₂ location, where it has access to its substrate. A generic lipid substrate is shown (black stick structure), but the substrate could also be a protein. (Bottom) A protein substrate (blue rod) is shown moving in response to cholesterol loading (black arrow) while the hydrolytic enzyme remains stationary. In (C), CRP activation is shown by lipid gating. An ion channel (blue shading) is localized to GM1 clusters, where it is held inactive from a lack of PIP₂. Disruption of GM1 lipids (black arrow) allows the channel to move to PIP₂ clusters where PIP₂ concentration is high. The binding of PIP₂ causes a conformational change in the transmembrane domain that opens the channel. In (D), CRP activation is shown by membrane thickness. An ion channel (blue shading) is sequestered into thick lipids (GM1 lipids). The thickness drives an inactive state. When the channel moves from GM1 lipids, the membrane thins, causing the helices to change conformation and open the channel.

Many ion channels, transporters, enzymes, and guanine-coupled protein receptors (GPCRs) are both palmitoylated and contain a PIP₂ binding site [13,24–26]. Where they localize can often influence protein function (Figure 1B–D). Until recently, detecting a protein moving between GM1 and PIP₂ was precluded by lacking a microscope with sufficient resolution [13].

In the absence of appropriate resolution, the movement of proteins between GM1 and PIP₂ domains went undetected. Studies of proteins localizing with lipids were limited to biophysical properties. For example, many proteins co-purify with GM1 lipids, and disrupting GM1 clusters alters protein function [27–29]. Similarly, PIP₂ was shown to bind directly to ion channels and transporters using structure determination [15,30–34]. PIP₂ also dramatically regulates protein function through protein–lipid interactions, including gating ion channels and trafficking membrane proteins [13–17,35–39]. Here we use these biophysical properties and recent findings from super-resolution imaging [7,22,40–43] to establish basic models for proteins moving nanoscopic distances in the membrane. We define

cholesterol-regulated proteins (CRPs) and their activation mechanism by CRP localization. A few recent examples of nanoscopic movement are provided, which may apply to multiple protein families needing further research. To help facilitate more research in this area, we will also discuss the techniques for labeling lipid compartments with super-resolution probes. We also describe the ability of super-resolution imaging to define the nanoscopic topology of membrane proteins with detail appropriate for a non-imaging expert.

2. CRP Activation

The movement of proteins' nanoscopic distances in the membrane is a potent mechanism by which a protein can be activated. A protein moving between lipids has the advantage that the concentration of a lipid substrate or ligand can remain constant in the membrane despite a dramatic change in the concentration experienced by the protein that moves [13,40]. The underlying premise relies only on membrane heterogeneity. Much of the heterogeneity is thought to arise from lipid clustering [10], but there are innumerable ways heterogeneity could arise in the membrane. For the purposes of this review, we will primarily focus on three nanoscopic locations of membrane heterogeneity: GM1 domains, PIP₂ domains, and disordered lipids. We will also focus on three mechanisms (substrate presentation, ligand presentation, and membrane thickness). We also note that microscopic movement (>250 nm) from the cytosol to the plasma membrane or from the cytosol to the nucleus have parallel mechanisms of substrate presentation; they are briefly mentioned but not discussed.

2.1. Substrate Presentation

Substrate presentation is a biological process that employs lipid domains/clusters to activate a protein by selectively exposing the protein to its substrate. In contrast to allosteric activation, the protein need not undergo a conformational change to be activated. The protein simply moves from a region of low substrate concentration to a region of high substrate concentration (Figure 1B). One of the first and best mechanisms for substrate presentation is phospholipase D2 (PLD2) [22]. PLD2 is palmitoylated, and the palmitoylation is responsible for the enzyme's localization with GM1 clusters and sensitivity to anesthetics [10,44]. The substrate for PLD2, phosphatidylcholine (PC), is primarily poly-unsaturated [45] and resides in the disordered region near PIP₂. When cholesterol is lowered, PLD2 leaves GM1 clusters and binds to PIP₂, where it finds its substrate and produces phosphatidic acid.

In a second type of substrate presentation, the enzyme is permanently clustered, and the substrate moves (Figure 1B, bottom panel). For example, in inflammation and Alzheimer's disease enzyme activation occurs with the substrate moving into GM1 clusters [46–52]. Specifically, the amyloid precursor protein (APP) is a substrate for gamma-secretase. The secretase remains clustered to GM1 lipids, and the substrate (APP) moves between GM1 and the disordered membrane region. When cholesterol is high, APP moves to gamma-secretase, where it is cleaved [41].

Classic inflammatory cytokines also work through a substrate movement mechanism. The cytokines are expressed as membrane proteins that reside in the disordered region. During an inflammatory response, cholesterol from the blood is taken up into the cell membrane [3,4]. The cholesterol causes the membrane-bound cytokines to move into GM1 clusters, where they encounter their hydrolytic enzymes. They are cleaved, and the soluble cytokine is released [42,53–56]. The affinity of the proteins for GM1 lipids is driven by a palmitate-GM1 interaction [11].

In the brain, astrocyte cholesterol regulates the amount of cholesterol available to neighboring cells. For example, astrocytes regulate the ability of neurons to produce amyloid proteins by releasing cholesterol, which is then transported to the neuron and taken up into the plasma membrane [41]. A similar process may occur for regulating cytokine production in microglia [42].

2.2. Ligand Presentation

Proteins partitioning into lipids can also rapidly expose a channel or transporter to a lipid ligand. PIP₂ is chief among the lipid ligands that gate or regulate ion transport proteins [14,15,17]. The same PIP₂ that localizes a protein to PIP₂ clusters also serves as a ligand that activates ion transport proteins, including ion channels [15,17,57–65]. Hence protein movement from a GM1 domain to a PIP₂ domain can also gate a channel (See Figure 1C), which we refer to here as “ligand presentation”. A good example of ligand presentation is the channel Twik-related potassium subtype 1 (TREK-1) which depends on its exposure to PIP₂ and local production of PA in the disordered region for its activation [12,40,66,67]. The lipids bind with ligand-like characteristics that gate the channel [18,68].

Cholesterol can have a similar but opposite effect as PIP₂ on localization. For example, inward rectifier potassium (K_{ir}) channels bind to cholesterol-rich GM1 lipids [69]. But K_{ir} isotype 2.1 (K_{ir}2.1) does not always remain in the GM1 clusters; rather, it moves between the two domains [70]. This has at least two consequences [71]. First, cholesterol has a binding site on K_{ir}2.1 that is believed to bind cholesterol directly and inhibit the channel [72]. Secondly, however, K_{ir}2.1 has a PIP₂ binding site that gates the channel [30]. As mentioned, GM1 clusters are separated spatially from PIP₂; hence when the channel is in a GM1 cluster, the concentration of its activating lipid PIP₂ is decreased. It is unclear which is more important, a lack of PIP₂ or direct inhibition by cholesterol. However, the combined effect of lipids appears to gate the channel, as the channel is inactive in high cholesterol [73].

In another example, PLD2 binds to TWIK-related potassium channel isotype 1 (TREK-1), producing local PA sufficient to activate the channel [67]. This appears to be an example where substrate presentation combines with lipid gating to activate a channel [66]. The PA binds TREK-1 with μ M affinity [68], and local production is estimated in the mM range near the enzyme before diffusion [13].

2.3. Membrane Thickness

Ordered lipids are thicker than disordered lipids by up to 10 Å [74–76]. When cholesterol increases in the membrane, the ordering of GM1 lipids increases, and the membrane becomes thicker [75,76] (Figure 1A). PIP₂ clusters reside within the disordered (thin) region of the membrane [20,22,23]; hence moving from GM1 clusters to PIP₂ clusters requires shifting from thick lipids to thin lipids. The concept of moving between lipids of different thicknesses as a protein activation mechanism was proposed for the gramicidin A channel using artificial membranes [77]. Figure 1D shows a hypothetical channel opening by shifting between membranes of differing thicknesses.

Supporting this model, many channels and transporters are bundles of alpha-helices that span the membrane. When the membrane thins, the helices will either create a hydrophobic mismatch, bend, or lay flat to accommodate the new hydrophobic boundary [78,79]. Structural examples of transmembrane thinning have been observed for bacterial mechanosensitive channels [80–82]. For example, early models of large prokaryotic mechanosensitive channel (MscL) openings involved the helices lying flat in the membrane, which allows the pore to expand and dilate [81]. Molecular dynamics studies indicate thinning contributes to the energetics of MscL opening [83].

Recent structural studies with cryoEM show the helices of the small prokaryotic mechanosensitive channel MscS also move horizontally to the plane of the membrane, resulting in a thinner transmembrane section [80,84]. Although bacteria do not have cholesterol, lipid partitioning in bacteria has been considered [85], and membrane thickness drives proteins into lipid compartments that reduce hydrophobic mismatch [86]. Hence, changes in lipid composition or stretch-induced changes in thickness could affect channel opening directly through the membrane.

In the mammalian cell, there are changes in both cholesterol and PIP₂. The affinity of long transmembrane helices for GM1 lipids increases with increasing membrane thickness [86], which should oppose PIP₂ affinity. Proteins that change conformation add an

independent state to the localization. The concentration of PIP₂ can also be decreased by flopping to the outer leaflet [39]. Additional research into these potential mechanisms is warranted.

3. Combination of Lipid and Protein Labeling Using Two-Color Super-Resolution Imaging

Currently, the best technique to locate a protein within a nanoscopic lipid domain is to label the protein and the lipids and compare their localization using super-resolution imaging. Two-color super-resolution imaging works advantageously with labeled lipids. The lipids are the most stable markers of lipid domain location. Labeling them avoids the uncertainty of a protein marker moving from changes in experimental conditions, particularly changes in cholesterol.

3.1. dSTORM

Direct stochastic optical reconstruction microscopy (dSTORM) is a technique that resolves structures below the diffraction limit of light (~250 nm) [87]. To achieve super-resolution, a single fluorophore is measured multiple times, and the center of a gaussian distribution is calculated [88]. The fluorophores used for dSTORM are switchable, i.e., they can be stochastically switched on and off. To measure an isolated fluorophore, only a small number of fluorophores are active at a time [89]. All stochastic methods use some variation of this method to achieve super-resolution.

Lipids can be directly labeled using antibodies and toxins conjugated to appropriate dSTORM-compatible fluorophores. GM1 lipids are typically labeled with fluorescent cholera toxin B (CTxB). PIP₂ domains are labeled with fluorescent anti-PIP₂ antibodies. For two-color dSTORM, the proteins are labeled pairwise with the lipids using compatible colors that do not spectrally overlap.

Figure 2A,B shows a strategy for monitoring the nanoscopic movement of proteins in a membrane. The technique works with cells or whole tissue [7,22,41,90]. For cultured cells, the tissue is grown in an imaging chamber. The cells are fixed, and the lipids and proteins are fluorescently labeled (Figure 2A,B).

Super-resolution imaging uses pair correlation to associate a protein with a lipid domain. Pair correlation in super-resolution imaging is similar to “co-localization” in traditional confocal microscopy. Super-resolution microscopes identify the location of individual molecules. A radius is calculated between molecules, and the molecules with pair correlation at the shortest radii are considered “co-localized”.

Typically, a condition is directly compared to a control, and one determines a ‘shift’ in co-localization. This is particularly convincing when a protein decreases its co-localization with GM1 lipids and increases its co-localization with PIP₂ [6,22]. This shows a shift from GM1 to PIP₂ lipids (Figure 2C–E).

The starting location of a protein is critical for understanding if it has moved or not. In most cases, the proteins need to be endogenously expressed. Over-expressed proteins can saturate the GM1 lipids and spill into the regions they would not otherwise occupy without activation. For example, over-expression of PLD dramatically activates TREK-1 [66,67]—presumably by spilling out into the disordered region where both the enzyme and TREK-1 are activated [22,66,91]. For obvious reasons, localizing a protein to the wrong membrane compartment could be determinantal to the purpose of the experiment. For example, the over-expression of ACE2 alters the interaction of SARS-CoV-2 with its hydrolytic enzymes [92]. In theory, over-expressed proteins can yield data directly opposite of reality. Data from endogenously expressed proteins are generally the most reliable.

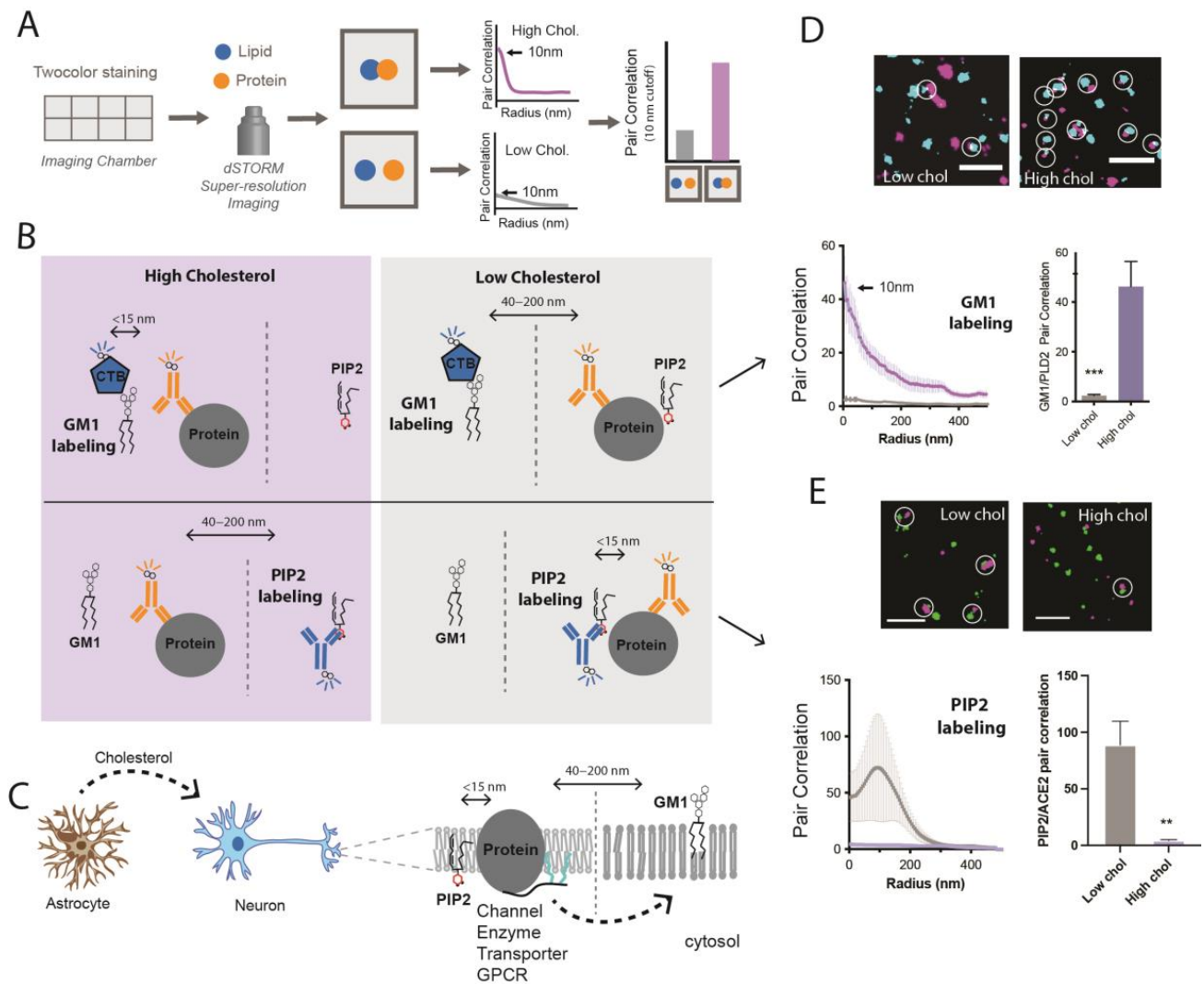


Figure 2. Strategy for detecting a protein moving between GM1 to PIP₂ clusters. (A) Labeling scheme and data analysis. Cells grown in 8-well imaging chambers are stained for a lipid and a protein and imaged with super-resolution. Hypothetical pair correlation data (proximity measurement) is shown. High pair correlation at short distances (e.g., 10 nm) indicates an association. (B) Strategy for establishing cholesterol-dependent localization. Each lipid compartment is labeled pairwise with protein in either high or low cholesterol. Typically, GM1 clusters and proteins are fluorescently labeled with Cholera Toxin B or antibody. (C) Model for CRP regulation in a neuron by astrocyte cholesterol. Astrocytes produce cholesterol which is transported to neurons with apolipoprotein E (ApoE). The neuron takes up the cholesterol into the plasma membrane, where it sequesters proteins with ordered GM1 lipids. (D) Pair correlation data of phospholipase D2 leaving a lipid raft after treating cells to remove cholesterol. Data adapted from Pavel et al., PNAS 2020 [40]. (E) Pair correlation data of angiotensin-converting enzyme 2 (ACE2) moving to PIP₂ domains after cholesterol removal. Adapted from Wang et al., 2020 [6]. ** $p < 0.01$ and *** $p < 0.001$.

3.2. Understanding Cholesterol's Role in Disease

Cholesterol's concentration in the membrane of cells can be adjusted up or down to determine whether a particular protein's association with a GM1 lipid is sensitive to cholesterol. As mentioned, cholesterol causes increased nematic order in the GM1 lipids. The order reduces fluidity in the ordered region. However, in the disordered region, cholesterol acts as a lubricant that untangles acyl chains and allows them to be more fluid [93]. In general, cholesterol combines to fluidize the membrane [10]. The effect of a protein moving to lipids and the fluidity changing are likely synergistic, but sorting out

the relative contributions to disease has been challenging. One of the biggest challenges is simply adjusting the cholesterol level in the cell membrane.

In the brain, astrocytes use apoE to control cholesterol loading into neurons [41,42]. The same apoE can be purified and added to cell cultures with and without a source of cholesterol to respectively load and unload cholesterol into cells [6,7,41,42]. PLD2 and ACE2 are an example of enzymes that move in and out of GM1 domains in a cholesterol-dependent manner (Figure 2D,E). A model for brain cholesterol-regulating protein localization is shown in Figure 2C.

3.3. PALM

Photo-activated localization microscopy (PALM) super-resolution imaging is a similar technique to dSTORM, which uses photoactivatable proteins. Using proteins allows for genetically encoding the fluorescent label needed for super-resolution [94]. Genetically encoded PIP₂ sensors are available for PALM imaging [43,95]. PIP₂ is typically measured on the inner leaflet of the plasma membrane, which is not accessible in live cells. Genetically encoded PIP₂ sensors have the advantage of visualizing the proteins without membrane permeabilization. Even in fixed cells, membrane permeabilization could be problematic since the membrane is what one intends to observe.

The genetically encoded PIP₂ sensors are comprised of the PLC- δ PIP₂ binding domain and a genetically encoded PALM protein. This technique was recently used to show the clustering of SARS-CoV-2 (SARS2) spike protein with PIP₂ [43,96]. The spike protein was genetically encoded with dendra2 and the PIP₂ binding domain from PLC- δ with PAMKate. Similar to dSTORM, the proteins have non-overlapping spectra, and they are suitable for cross-pair correlation analysis.

Similar to the PALM study, SARS-CoV-2 viral entry was studied with dSTORM looking at the viral receptor angiotensin-converting enzyme 2 (ACE2) co-localization with PIP₂ [7]. Since the spike protein binds to the ACE2 receptor, the two studies provide the best comparison of dSTORM in fixed cells with PALM in live cells. Using live cell PALM, the PIP₂ cluster sizes appeared larger than in similar studies done in fixed cells [7,95]. Nonetheless, both studies confirm the power of super-resolution imaging to visualize the nanoscopic location of viral entry.

4. The Palmitate Binding Site

The affinity of proteins to GM1 lipids depends on palmitate binding to saturated ceramides of GM1 lipids [11]. Kai Simons produced early data showing a protein's affinity for lipids using detergent-resistant membranes [44]. The Tsien lab used palmitoylation combined with genetically encoded FRET partners to detect movement in and out of GM1 clusters in a biological membrane [96].

The mechanism of palmitate affinity is based on nematic order [11,97–99]. Like proteins, lipids have regions of order and disorder [10]. The ordered GM1 structures are formed from saturated ceramides that orient perpendicular to the surface of the membrane. Once ordered, they provide an energetically favorable binding surface/pocket for palmitate (Figure 3A). Palmitate is a saturated 16-carbon lipid. When extended, the saturated carbons match the surface and maximize Van der Waals interactions (Figure 3A). In cells, the lipid is naturally covalently attached to proteins in a process called palmitoylation. The palmitoylated proteins are localized to GM1 lipids by the lipid-lipid interaction. A covalently attached myristate (14-carbon saturated lipid) has a similar effect [100].

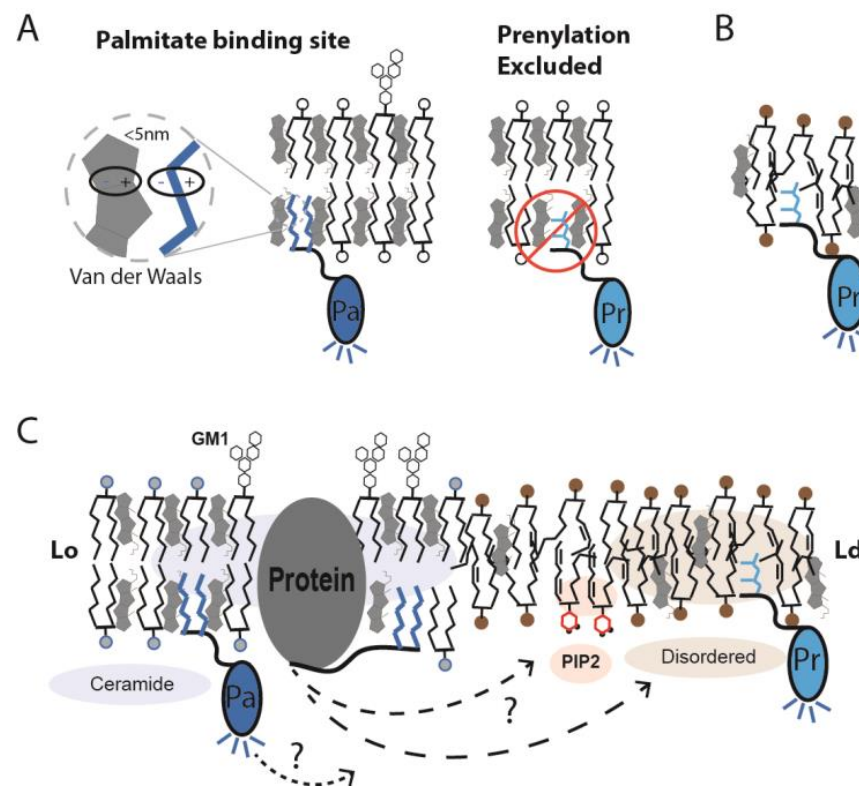


Figure 3. Palmitate binding site in ordered lipids. (A) A model depicting the molecular basis for GM1 lipids selectively binding to palmitoylated protein (Pa). GM1 lipids are saturated and pack well with cholesterol and palmitate. The site is specific and does not bind prenylated (Pr) proteins. The branched structure of prenyl lipids is thought to clash with the structured palmitate site, thus excluding prenylated proteins from ordered lipid domains (Lo). When attached to a fluorescent protein (dark blue shaded protein), the palmitoylation becomes a sensor for the order of GM1 lipids. (B) The prenylation binding site is shown within disordered lipids (unsaturated with bent acyl chains). When coupled to a genetically encoded fluorescent protein (light blue shading), the prenylated protein functions as a sensor of prenyl localization. (C) In cellular membranes, the covalent attachment of a palmitate or a prenyl lipid to a protein tags the protein for sorting between GM1 and disordered lipids, respectively. If the protein is a fluorescent protein, the respective compartments are fluorescently labeled. (B) When the order of the GM1 lipids is decreased, the palmitate binding site is disrupted, and the palmitoylated proteins can move away from the GM1 lipids. Some proteins move to PIP₂ clusters (red shading), some move to disordered lipids (tan shading), and some proteins may remain clustered with GM1. Without labeling the lipid, the movement of proteins between lipids is unclear, as depicted by a '?' in the figure.

Prenylation is a second type of lipid modification that attaches a branched unsaturated lipid. The branching is incompatible with the rigid flat surface of the cholesterol. Hence, a protein with a prenyl group is excluded from the ordered GM1 domain. This was first shown by FRET [96] and, more recently, with super-resolution imaging [90].

The selectivity of the palmitate binding site is remarkable and experimentally demonstrates that the order is present in the lipids. If the cell were homogenous, there would be no separation of the two lipid modifications. In the cell, these post-translational modifications serve as localization tags that separate proteins. For additional understanding of lipidation, we refer the reader to basic reviews on palmitoylation [100,101] and prenylation [102,103].

Lipid order is not to be confused with lipid partitioning. Lipid partitioning separates saturated and unsaturated lipids to form separate domains, but the partitioning does not necessarily create order within the domains. Lipid order is dictated by the structure of the lipids and proteins within a particular domain. The ordered palmitate binding site exists in pure saturated lipids, absent any partitioning.

The palmitoylated probes are suitable for studying the state or function of the GM1 cluster. Through understanding the function of the domain, one can begin to predict how the palmitoylation affects the association of a protein with GM1 clusters. However, the palmitoylated probes do not typically reveal how individual proteins function in the GM1 clusters. The reason being many proteins have both palmitoylation and PIP₂ binding sites. Hence, a protein can shift between the domains based on PIP₂ levels independent of cholesterol's effect on palmitoylation. Furthermore, some proteins may not be palmitoylated; rather, they bind to a palmitoylated protein. For example, TREK-1 is not palmitoylated, but it binds phospholipase D2, which is palmitoylated [22,67].

The thickness of a protein also directs its localization [86]. And as mentioned previously, proteins undergo conformational changes that affect their membrane thickness. Cleavage of a transmembrane helix in the membrane can also affect its thickness. Hence, the location of a protein depends on many factors independent of palmitoylation. Thus, a palmitoylation probe alone is insufficient for predicting how a protein will interact with GM1 clusters. Furthermore, the palmitoylation and prenylation probes do not indicate a direct association with PIP₂ or other lipids that may cluster proteins.

5. Strengths and Weaknesses of Imaging Techniques

Directly labeling proteins and lipids has advantages over lipidated probes. When the cholesterol is lowered, palmitoylated proteins tend to leave lipid rafts [6,7,41]. Hence, a probe will leave and no longer report the localization of a protein with a GM1 domain. This is a problem for both the FRET probes and the dSTORM probes described previously. For example, when PLD2 disassociates with a GM1 cluster, it could end up in the disordered region with the probe, which could cause confusion. If the protein happens to bind PIP₂, the probe and the protein will be separated, but only because the probe does not bind PIP₂, not because the probe is marking the GM1 domain (Figure 3C).

As additional proteins are identified that remain in the lipid rafts, those proteins may serve as resident markers. For example, gamma-secretase is cholesterol independent and appears to remain in lipid rafts under any condition. In contrast, its substrate APP moves in and out of lipid rafts as astrocytes raise and lower (respectively) the cholesterol [41]. Other proteins like clathrin and flotillin are also very good candidates for marking the lipid compartments. However, there will always be the risk that, in a new condition, a protein marker leaves the lipid raft. The only way to know the lipid location for sure will be to label the endogenous lipids and the protein of interest.

A background reduction is one advantage of super-resolution imaging. The background is lowered by quantitating the labeling only in the proximity of the protein of interest (Figure 4A). Often endogenous proteins are expressed at very low levels. A low signal inevitably leads to high background. With super-resolution imaging, noise is excluded by looking at very short distances. Proteins are around 5 nm in diameter. A protein bound directly to another protein should be within 5–10 nm. Proteins that are 50 and 100 nm away are not co-localized. The probability that background labeling is within 5–10 nm is very low under normal protein densities (see Figure 4A for an illustration). Hence, the random association of background at short distances is only significant when the background concentration is very high.

The precision of the dSTORM instrument is around 5–10 nm depending on the cell type and the labeling. Figure 4B shows dSTORM precision data from 4 cell types (data taken from previous publications under open source license [7]). In practice, a precision of 5–10 nm is a sufficiently short radius so that background observations have a reduced impact on results from pair correlation analysis.

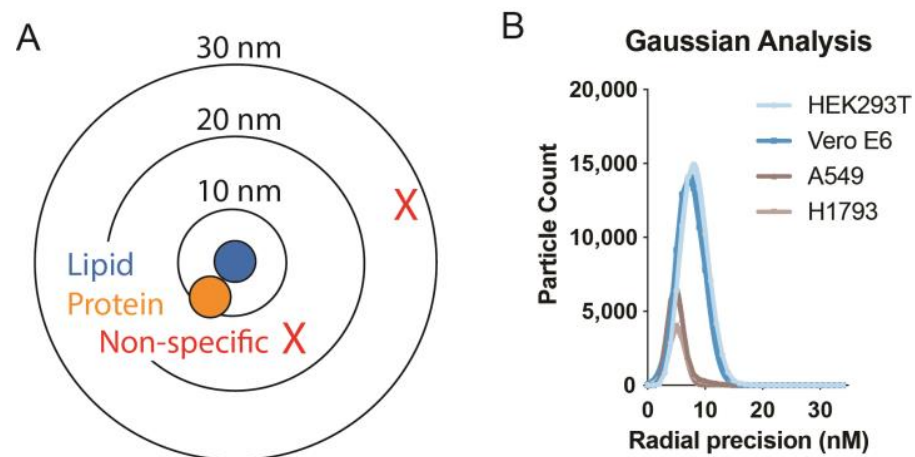


Figure 4. Non-specific labeling in two-color dSTORM. (A) The bin size in radius (10, 20, and 30 nm) is drawn at scale. Proteins (orange, <5 nm in diameter) can associate with a lipid (blue shading). Non-specific labeling (red X) occurs randomly and does not typically associate directly with the lipid or protein. When a radius of 5–10 nm is used, the random background is excluded from the measurement by virtue of proximity. The shorter the distance, the more background is excluded allowing pair correlation for low abundant proteins or those with a high background. (B) Example of precision measurements from a dSTORM super-resolution instrument (Vutara VXL). The cells were stained for GM1 and PIP₂ lipids. Radial precisions in 4 different cell types varied between 4 and 8 nm. Hence very little random overlap occurs due to precision above 10 nm. Taken from Yuan et al., 2022 with permission [7].

One weakness of the PALM method is the over-expression of the PIP₂ sensor. The sensor has high affinity and logically should compete with proteins that transiently bind to PIP₂. Theoretically, this should drive PIP₂ binding proteins to associate more with GM1 lipids. A second weakness is the over-expression of the proteins of interest. Over-expression can saturate the lipid raft and cause the over-expressed protein to spill into an unregulated region. For example, phospholipase D2 (PLD2), which is inactivated by sequestration into lipid rafts, is activated by over-expression. Over-expression alone significantly increases PLD2 activity and TREK-1 currents [67,104]. Expressing genetically encoded proteins under endogenous promoters will alleviate this problem.

Some consideration needs to be given to artificial clustering by antibodies and CTxB. Even in fixed cells, lipids appear mobile over short distances, especially saturated lipids [105]. For lipids like GM1 that cluster on their own, pentadentate binding of the sugar head groups can lead to additional clustering. The clustering affects the cluster size but does not appear to contribute much to function. As mentioned, the function of GM1 lipids is based on the binding palmitate, which is dictated by the ordering of the lipid, not the size of the cluster per se. This is evident from anesthetic treatments which disrupt the order while increasing the cluster size [40]. At microscopic distances, measured by fluorescence recovery after photobleaching (FRAP), cholera toxin-labeled GM1 lipids appear relatively immobile [12].

Some artificial clustering, especially at short distances, can improve pair correlation by creating more distinct clusters. Prior to super-resolution imaging, Reinhard Jahn developed a technique called antibody patching [106] to determine the co-localization of proteins. Antibody patching uses antibodies to create protein clusters discernable by a confocal microscope. Proteins that were associated were driven into the same clusters, and proteins that were not associated were separated by the clustering (see Figure 5A, data reproduced with permission).

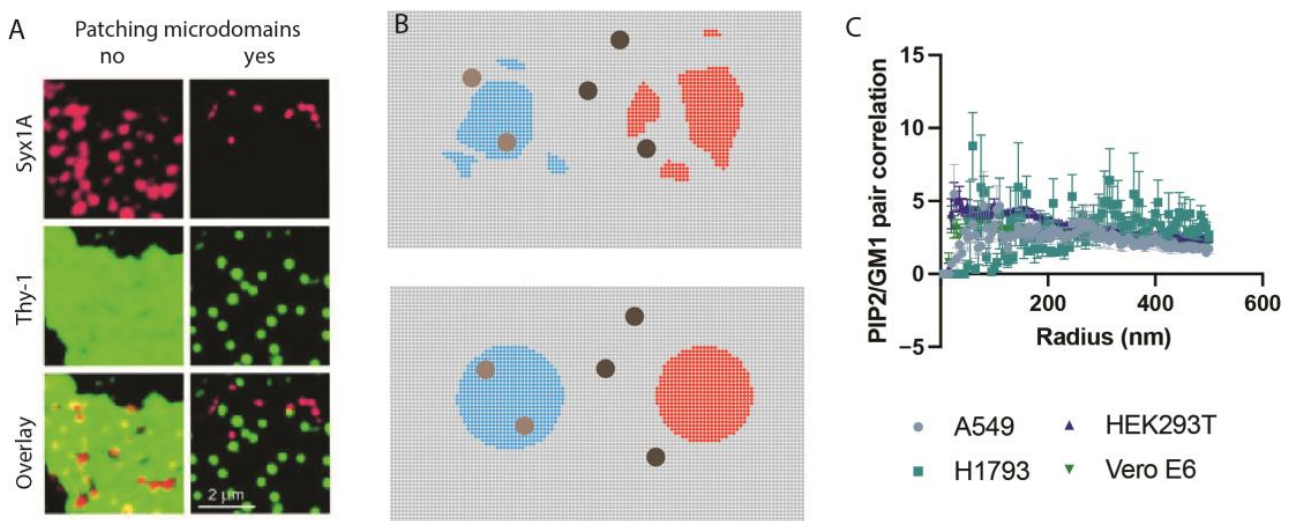


Figure 5. Antibody patching. (A) antibody patching in unfixed cells. Patches can be seen without super-resolution imaging. Adapted from Lang et al., 2001 with permission [107]. (B) Depiction of antibody patching at nanoscopic levels. In the top panel, there are multiple patches of different sizes. In the bottom panel, clustering helps create lipid domains of more uniform size which is important to the cluster analysis. In light blue, the clustering pulls together proteins more associated with the lipid domains. In red, the clustering separates proteins less associated with the lipid domains. (C) Pair correlation of PIP₂ with GM1 in multiple cell types. Pair correlation is very low, suggesting PIP₂ and GM1 lipids are separate. A549 are lung epithelial, Human embryonic kidney (HEK293), Vero E6 monkey kidney, and H1793 lung epithelial. Data adapted from Yuan et al., 2022 with permission [7].

In theory, the antibody patch principle should work for super-resolution microscopy. Figure 5B shows a hypothetical enhanced clustering of GM1 and PIP₂. The proteins are first fixed and then stained with cholera toxin B (CTxB). This allows for limited artificial clustering of the saturated lipids (the marker) while avoiding artificial clustering of palmitoylated proteins (the protein of interest). From experimentation, the average lipid cluster size is typically <200 nm after fixing [7,22,40–42], demonstrating that any clustering of lipids is limited to nanoscopic distances.

6. Future Directions

Going forward, nanoscopic topology and its dynamic function must be considered for all classes of palmitoylated and PIP₂ binding proteins. As mentioned, many classes of ion channels and transporters are palmitoylated [24], and many channels and transporters are regulated by PIP₂. GPCRs have palmytoilation in all their alpha subunits, prenylation in all their G-beta gamma subunits, and a putative PIP₂ binding site in the GPCR [26]. Their role in CRP activation is largely unknown.

Labels for additional compartments also need to be developed. PIP₃ appears to reside separately from PIP₂ and GM1 [23]. Lipid-gated Ion channels and several transporters respond differently to PIP₂ and PIP₃ [15]. The relative concentrations are important as PTEN is an enzyme that converts PIP₃ to PIP₂, and mutation contributes to autism [107].

It is unclear whether PIP₃ partitions into a separate compartment or is maintained separately through its local production and degradation. Early mass spec studies suggested that PIP₃ contains short-chain saturated lipids vs. long-chain unsaturation in PIP₂ [15]. Hence the lipids could partition based on lipid hydrophobicity. However, the separation could be generated independently of lipid partitioning or by flopping to the outer leaflet [39]. One speculative mechanism might involve local production near an enzyme. As the lipid is generated, it will be highest near its metabolic enzymes.

The separation of PIP₂ and GM1 is still somewhat controversial. Early studies found PIP₂ in pull-down experiments with detergent-resistant membranes (DRMs) [108]. This led

investigators to conclude that PIP₂ resides in lipid rafts. However, the association of PIP₂ to GM1 lipids through proteins that bind both lipids was not considered. Some percentage of DRM proteins will have PIP₂ bound, and if there are lots of proteins that bind both PIP₂ and GM1, there could be a significant amount of PIP₂ associated with DRMs. Early indirect experiments support a distinct location for PIP₂ [109].

The most reliable experiment for testing PIP₂ and GM1 co-localization is super-resolution imaging in the intact membrane. Three groups labeled the membrane and found that GM1 and PIP₂ appeared separated. Figure 5C shows pair correlation from 4 cell lines with little to no pair correlation. No group using super-resolution imaging has concluded that significant PIP₂ resides in GM1 clusters. Furthermore, PIP₂ is arachidonylated, so there is no chemical basis for PIP₂ being associated with ordered GM1 lipids. PIP₂ should be excluded from lipid rafts for the same reasons prenylated proteins are excluded. As more proteins emerge that use movement between lipid rafts and PIP₂ as their activation mode, this GM1/PIP₂ paradigm will continue solidifying. While speculative at this point, some proteins that have very high affinities for PIP₂ may attract PIP₂ into GM1 clusters. This would tend to disrupt the lipid order, but would not necessarily be true of detergent-resistant membranes. Once the membrane is disrupted by detergent, proteins associated with GM1 lipids may also bind the dispersed PIP₂.

In conclusion, the extent of CRP localization is scarcely known. The number of proteins regulated by cholesterol and nanoscopic movement is likely extensive and integral to many diseases where cholesterol levels are known to be important. Having the right tools to investigate the mechanisms is critical and will likely continue to improve as the technology expands through the ion transport and enzyme communities.

Funding: This work was supported by a Director's New Innovator Award to S.B.H. (DP2NS087943), an R01 (R01NS112534) from the National Institutes of Health.

Institutional Review Board Statement: Not applicable.

Informed Consent Statement: Not applicable.

Data Availability Statement: Not applicable.

Acknowledgments: We thank Andrew S. Hansen for reading the manuscript and for helpful suggestions.

Conflicts of Interest: The authors declare no competing interests.

References

1. Puglielli, L.; Tanzi, R.E.; Kovacs, D.M. Alzheimer's disease: The cholesterol connection. *Nat. Neurosci.* **2003**, *6*, 345–351. [[CrossRef](#)] [[PubMed](#)]
2. Wolozin, B. Cholesterol and the Biology of Alzheimer's Disease. *Neuron* **2004**, *41*, 7–10. [[CrossRef](#)]
3. Tall, A.R.; Yvan-Charvet, L. Cholesterol, inflammation and innate immunity. *Nat. Rev. Immunol.* **2015**, *15*, 104–116. [[CrossRef](#)] [[PubMed](#)]
4. Luo, J.; Yang, H.; Song, B.-L. Mechanisms and regulation of cholesterol homeostasis. *Nat. Rev. Mol. Cell Biol.* **2020**, *21*, 225–245. [[CrossRef](#)] [[PubMed](#)]
5. Kapadia, S.B.; Barth, H.; Baumert, T.; McKeating, J.A.; Chisari, F.V. Initiation of Hepatitis C Virus Infection Is Dependent on Cholesterol and Cooperativity between CD81 and Scavenger Receptor B Type I. *J. Virol.* **2007**, *81*, 374–383. [[CrossRef](#)]
6. Wang, H.; Yuan, Z.; Pavel, M.A.; Hansen, S.B. The role of high cholesterol in age-related COVID19 lethality. *bioRxiv* **2020**. [[CrossRef](#)]
7. Yuan, Z.; Pavel, M.A.; Wang, H.; Kwachukwu, J.C.; Mediouni, S.; Jablonski, J.A.; Nettles, K.W.; Reddy, C.B.; Valente, S.T.; Hansen, S.B. Hydroxychloroquine blocks SARS-CoV-2 entry into the endocytic pathway in mammalian cell culture. *Commun. Biol.* **2022**, *5*, 1–12. [[CrossRef](#)]
8. Cardoso, D.; Perucha, E. Cholesterol metabolism: A new molecular switch to control inflammation. *Clin. Sci.* **2021**, *135*, 1389–1408. [[CrossRef](#)] [[PubMed](#)]
9. Kabir, H.A.; Hashmi, K.A. Non-HDL Cholesterol as a Predictor of Cardiovascular Disease in Type 2 Diabetes. *Med. Forum Mon.* **2021**, *32*, 68–71.
10. Sezgin, E.; Levental, I.; Mayor, S.; Eggeling, C. The mystery of membrane organization: Composition, regulation and roles of lipid rafts. *Nat. Rev. Mol. Cell Biol.* **2017**, *18*, 361–374. [[CrossRef](#)]

11. Levental, I.; Lingwood, D.; Grzybek, M.; Coskun, U.; Simons, K. Palmitoylation regulates raft affinity for the majority of integral raft proteins. *Proc. Natl. Acad. Sci. USA* **2010**, *107*, 22050–22054. [[CrossRef](#)] [[PubMed](#)]
12. Petersen, E.N.; Pavel, M.A.; Wang, H.; Hansen, S.B. Disruption of palmitate-mediated localization; a shared pathway of force and anesthetic activation of TREK-1 channels. *Biochim. Biophys. Acta Biomembr.* **2019**, *1862*, 183091. [[CrossRef](#)]
13. Robinson, C.V.; Rohacs, T.; Hansen, S.B. Tools for Understanding Nanoscale Lipid Regulation of Ion Channels. *Trends Biochem. Sci.* **2019**, *44*, 795–806. [[CrossRef](#)] [[PubMed](#)]
14. Suh, B.-C.; Hille, B. PIP₂ Is a Necessary Cofactor for Ion Channel Function: How and Why? *Annu. Rev. Biophys.* **2008**, *37*, 175–195. [[CrossRef](#)]
15. Hansen, S.B. Lipid agonism: The PIP₂ paradigm of ligand-gated ion channels. *Biochim. Biophys. Acta Mol. Cell Biol. Lipids* **2015**, *1851*, 620–628. [[CrossRef](#)]
16. Logothetis, D.E.; Petrou, V.I.; Adney, S.K.; Mahajan, R. Channelopathies linked to plasma membrane phosphoinositides. *Eur. J. Physiol.* **2010**, *460*, 321–341. [[CrossRef](#)] [[PubMed](#)]
17. Hilgemann, D.W.; Feng, S.; Nasuhoglu, C. The Complex and Intriguing Lives of PIP₂ with Ion Channels and Transporters. *Sci. Signal.* **2001**, *2001*, re19. [[CrossRef](#)]
18. Schrecke, S.; Zhu, Y.; McCabe, J.W.; Bartz, M.; Packianathan, C.; Zhao, M.; Zhou, M.; Russell, D.; Laganowsky, A. Selective regulation of human TRAAK channels by biologically active phospholipids. *Nat. Chem. Biol.* **2020**, *17*, 89–95. [[CrossRef](#)]
19. Han, K.; Kim, S.H.; Venable, R.M.; Pastor, R.W. Design principles of PI(4,5)P₂ clustering under protein-free conditions: Specific cation effects and calcium-potassium synergy. *Proc. Natl. Acad. Sci. USA* **2022**, *119*, e2202647119. [[CrossRef](#)]
20. Bogaart, G.V.D.; Meyenberg, K.; Risselada, H.J.; Amin, H.; Willig, K.I.; Hubrich, B.E.; Dier, M.; Hell, S.W.; Grubmüller, H.; Diederichsen, U.; et al. Membrane protein sequestering by ionic protein–lipid interactions. *Nature* **2011**, *479*, 552–555. [[CrossRef](#)] [[PubMed](#)]
21. Levental, I.; Christian, D.A.; Wang, Y.-H.; Madara, J.J.; Discher, D.E.; Janmey, P.A. Calcium-Dependent Lateral Organization in Phosphatidylinositol 4,5-Bisphosphate (PIP₂) and Cholesterol-Containing Monolayers. *Biochemistry* **2009**, *48*, 8241–8248. [[CrossRef](#)] [[PubMed](#)]
22. Petersen, E.N.; Chung, H.-W.; Nayeboadri, A.; Hansen, S.B. Kinetic disruption of lipid rafts is a mechanosensor for phospholipase D. *Nat. Commun.* **2016**, *7*, 13873. [[CrossRef](#)] [[PubMed](#)]
23. Wang, J.; Richards, D.A. Segregation of PIP₂ and PIP₃ into distinct nanoscale regions within the plasma membrane. *Biol. Open* **2012**, *1*, 857–862. [[CrossRef](#)]
24. Shipston, M.J. Ion Channel Regulation by Protein Palmitoylation. *J. Biol. Chem.* **2011**, *286*, 8709–8716. [[CrossRef](#)]
25. Escribá, P.V.; Wedegaertner, P.B.; Goñi, F.M.; Vögler, O. Lipid–protein interactions in GPCR-associated signaling. *Biochim. Biophys. Acta Biomembr.* **2007**, *1768*, 836–852. [[CrossRef](#)]
26. Damian, M.; Louet, M.; Gomes, A.A.S.; M’Kadmi, C.; Denoyelle, S.; Cantel, S.; Mary, S.; Bisch, P.M.; Fehrentz, J.-A.; Catoire, L.J.; et al. Allosteric modulation of ghrelin receptor signaling by lipids. *Nat. Commun.* **2021**, *12*, 3938. [[CrossRef](#)]
27. Romanenko, V.G.; Fang, Y.; Byfield, F.; Travis, A.J.; Vandenberg, C.A.; Rothblat, G.H.; Levitan, I. Cholesterol Sensitivity and Lipid Raft Targeting of Kir2.1 Channels. *Biophys. J.* **2004**, *87*, 3850–3861. [[CrossRef](#)]
28. Szőke, É.; Börzsei, R.; Tóth, D.M.; Lengl, O.; Helyes, Z.; Sándor, Z.; Szolcsányi, J. Effect of lipid raft disruption on TRPV1 receptor activation of trigeminal sensory neurons and transfected cell line. *Eur. J. Pharmacol.* **2010**, *628*, 67–74. [[CrossRef](#)]
29. Startek, J.B.; Ghosh, D.; Alpizar, Y.A.; López-Requena, A.; Van Ranst, N.; Voets, T.; Talavera, K. The Role of Lipid Rafts in the Localization and Function of the Chemosensory TRPA1 Channel. *Biophys. J.* **2016**, *110*, 26a. [[CrossRef](#)]
30. Hansen, S.B.; Tao, X.; MacKinnon, R. Structural basis of PIP₂ activation of the classical inward rectifier K⁺ channel Kir2.2. *Nature* **2011**, *477*, 495–498. [[CrossRef](#)]
31. Gao, Y.; Cao, E.; Julius, D.; Cheng, Y. TRPV1 structures in nanodiscs reveal mechanisms of ligand and lipid action. *Nature* **2016**, *534*, 347–351. [[CrossRef](#)] [[PubMed](#)]
32. Sun, J.; MacKinnon, R. Structural Basis of Human KCNQ1 Modulation and Gating. *Cell* **2019**, *180*, 340–347.e9. [[CrossRef](#)] [[PubMed](#)]
33. Anderluh, A.; Hofmaier, T.; Klotzsch, E.; Kudlacek, O.; Stockner, T.; Sitte, H.H.; Schütz, G.J. Direct PIP₂ binding mediates stable oligomer formation of the serotonin transporter. *Nat. Commun.* **2017**, *8*, 14089. [[CrossRef](#)] [[PubMed](#)]
34. Laverty, D.; Desai, R.; Uchański, T.; Masiulis, S.; Stec, W.J.; Malinauskas, T.; Zivanov, J.; Pardon, E.; Steyaert, J.; Miller, K.W.; et al. Cryo-EM structure of the human $\alpha 1\beta 3\gamma 2$ GABAA receptor in a lipid bilayer. *Nature* **2019**, *565*, 516–520. [[CrossRef](#)] [[PubMed](#)]
35. Song, W.; Sansom, M.S. Lipid-Dependent Regulation of Ion Channels and G Protein–Coupled Receptors: Insights from Structures and Simulations. *Annu. Rev. Pharmacol. Toxicol.* **2020**, *60*, 31–50. [[CrossRef](#)]
36. Phillips, R.; Ursell, T.; Wiggins, P.; Sens, P. Emerging roles for lipids in shaping membrane-protein function. *Nature* **2009**, *459*, 379–385. [[CrossRef](#)]
37. Grouleff, J.; Irudayam, S.J.; Skeby, K.K.; Schiøtt, B. The influence of cholesterol on membrane protein structure, function, and dynamics studied by molecular dynamics simulations. *Biochim. Biophys. Acta Biomembr.* **2015**, *1848*, 1783–1795. [[CrossRef](#)] [[PubMed](#)]
38. Harraz, O.F.; Hill-Eubanks, D.; Nelson, M.T. PIP₂: A critical regulator of vascular ion channels hiding in plain sight. *Proc. Natl. Acad. Sci. USA* **2020**, *117*, 20378–20389. [[CrossRef](#)]

39. Gulshan, K.; Brubaker, G.; Conger, H.; Wang, S.; Zhang, R.; Hazen, S.L.; Smith, J.D. PI(4,5)P₂ Is Translocated by ABCA1 to the Cell Surface Where It Mediates Apolipoprotein A1 Binding and Nascent HDL Assembly. *Circ. Res.* **2016**, *119*, 827–838. [[CrossRef](#)]
40. Pavel, M.A.; Petersen, E.N.; Wang, H.; Lerner, R.A.; Hansen, S.B. Studies on the mechanism of general anesthesia. *Proc. Natl. Acad. Sci. USA* **2020**, *117*, 13757–13766. [[CrossRef](#)]
41. Wang, H.; Kulas, J.A.; Holtzman, D.M.; Ferris, H.A.; Hansen, S.B. Regulation of beta-amyloid production in neurons by astrocyte-derived cholesterol. *Proc. Natl. Acad. Sci. USA* **2021**, *118*, e2102191118. [[CrossRef](#)]
42. Wang, H.; Kulas, J.A.; Higginbotham, H.; Kovacs, M.A.; Ferris, H.A.; Scott, B.; Hansen, S.B. Regulation of Neuroinflammation by Astrocyte-Derived Cholesterol. *bioRxiv* **2022**, *2*, e520161. [[CrossRef](#)]
43. Raut, P.; Waters, H.; Zimmerberg, J.; Obeng, B.; Gosse, J.; Hess, S.T. Localization-based super-resolution microscopy reveals relationship between SARS-CoV2 spike and phosphatidylinositol (4,5): Biphosphate. *Multiphoton Microsc. Biomed. Sci.* **2022**, *1196503*, e2613460. [[CrossRef](#)]
44. Lingwood, D.; Simons, K. Lipid Rafts as a Membrane-Organizing Principle. *Science* **2009**, *327*, 46–50. [[CrossRef](#)] [[PubMed](#)]
45. Gil Oliveira, T.; Chan, R.B.; Tian, H.; Laredo, M.; Shui, G.; Staniszewski, A.; Zhang, H.; Wang, L.; Kim, T.-W.; Duff, K.E.; et al. Phospholipase D2 Ablation Ameliorates Alzheimer’s Disease-Linked Synaptic Dysfunction and Cognitive Deficits. *J. Neurosci.* **2010**, *30*, 16419–16428. [[CrossRef](#)] [[PubMed](#)]
46. Bhattacharyya, R.; Barren, C.; Kovacs, D.M. Palmitoylation of Amyloid Precursor Protein Regulates Amyloidogenic Processing in Lipid Rafts. *J. Neurosci.* **2013**, *33*, 11169–11183. [[CrossRef](#)] [[PubMed](#)]
47. Hicks, D.A.; Nalivaeva, N.N.; Turner, A.J. Lipid Rafts and Alzheimer’s Disease: Protein-Lipid Interactions and Perturbation of Signaling. *Front. Physiol.* **2012**, *3*, 189. [[CrossRef](#)]
48. Hooper, N.M.; Rushworth, J.V. Lipid Rafts: Linking Alzheimer’s Amyloid- β Production, Aggregation, and Toxicity at Neuronal Membranes. *Int. J. Alzheimers Dis.* **2011**, *2011*, e603052.
49. Vetrivel, K.S.; Thinakaran, G. Membrane rafts in Alzheimer’s disease beta-amyloid production. *Biochim. Biophys. Acta Mol. Cell Biol. Lipids* **2010**, *1801*, 860–867. [[CrossRef](#)] [[PubMed](#)]
50. Cheng, H.; Vetrivel, K.S.; Gong, P.; Meckler, X.; Parent, A.; Thinakaran, G. Mechanisms of Disease: New therapeutic strategies for Alzheimer’s disease—Targeting APP processing in lipid rafts. *Nat. Clin. Pract. Neurol.* **2007**, *3*, 374–382. [[CrossRef](#)] [[PubMed](#)]
51. Cordy, J.M.; Hooper, N.; Turner, A.J. The involvement of lipid rafts in Alzheimer’s disease (Review). *Mol. Membr. Biol.* **2006**, *23*, 111–122. [[CrossRef](#)]
52. Ehehalt, R.; Keller, P.; Haass, C.; Thiele, C.; Simons, K. Amyloidogenic processing of the Alzheimer β -amyloid precursor protein depends on lipid rafts. *J. Cell Biol.* **2003**, *160*, 113–123. [[CrossRef](#)] [[PubMed](#)]
53. Miller, Y.I.; Navia-Pelaez, J.M.; Corr, M.; Yaksh, T.L. Lipid rafts in glial cells: Role in neuroinflammation and pain processing. *J. Lipid Res.* **2020**, *61*, 655–666. [[CrossRef](#)] [[PubMed](#)]
54. Varshney, P.; Yadav, V.; Saini, N. Lipid rafts in immune signalling: Current progress and future perspective. *Immunology* **2016**, *149*, 13–24. [[CrossRef](#)]
55. Koseki, M.; Hirano, K.-I.; Masuda, D.; Ikegami, C.; Tanaka, M.; Ota, A.; Sandoval, J.C.; Nakagawa-Toyama, Y.; Sato, S.B.; Kobayashi, T.; et al. Increased lipid rafts and accelerated lipopolysaccharide-induced tumor necrosis factor- α secretion in Abca1-deficient macrophages. *J. Lipid Res.* **2007**, *48*, 299–306. [[CrossRef](#)]
56. Fessler, M.B.; Parks, J.S. Intracellular Lipid Flux and Membrane Microdomains as Organizing Principles in Inflammatory Cell Signaling. *J. Immunol.* **2011**, *187*, 1529–1535. [[CrossRef](#)] [[PubMed](#)]
57. Yue, G.; Malik, B.; Yue, G.; Eaton, D. Phosphatidylinositol 4,5-Bisphosphate (PIP₂) Stimulates Epithelial Sodium Channel Activity in A6 Cells. *J. Biol. Chem.* **2002**, *277*, 11965–11969. [[CrossRef](#)]
58. Pian, P.; Bucchi, A.; DeCostanzo, A.; Robinson, R.B.; Siegelbaum, S.A. Modulation of cyclic nucleotide-regulated HCN channels by PIP₂ and receptors coupled to phospholipase C. *Pflugers Arch.* **2007**, *455*, 125–145. [[CrossRef](#)]
59. Suh, B.-C.; Hille, B. Recovery from Muscarinic Modulation of M Current Channels Requires Phosphatidylinositol 4,5-Bisphosphate Synthesis. *Neuron* **2002**, *35*, 507–520. [[CrossRef](#)]
60. Suh, B.-C.; Inoue, T.; Meyer, T.; Hille, B. Rapid Chemically Induced Changes of PtdIns(4,5)P₂ Gate KCNQ Ion Channels. *Science* **2006**, *314*, 1454–1457. [[CrossRef](#)]
61. Winks, J.S.; Hughes, S.; Filippov, A.K.; Tatulian, L.; Abogadie, F.C.; Brown, D.A.; Marsh, S.J. Relationship between Membrane Phosphatidylinositol-4,5-Bisphosphate and Receptor-Mediated Inhibition of Native Neuronal M Channels. *J. Neurosci.* **2005**, *25*, 3400–3413. [[CrossRef](#)] [[PubMed](#)]
62. Zhang, M.; Meng, X.-Y.; Cui, M.; Pascal, J.M.; E Logothetis, D.; Zhang, J.-F. Selective phosphorylation modulates the PIP₂ sensitivity of the CaM-SK channel complex. *Nat. Chem. Biol.* **2014**, *10*, 753–759. [[CrossRef](#)] [[PubMed](#)]
63. Nilius, B.; Owsianik, G.; Voets, T. Transient receptor potential channels meet phosphoinositides. *EMBO J.* **2008**, *27*, 2809–2816. [[CrossRef](#)] [[PubMed](#)]
64. Velisetty, P.; Borbiri, I.; Kasimova, M.A.; Liu, L.; Badheka, D.; Carnevale, V.; Rohacs, T. A molecular determinant of phosphoinositide affinity in mammalian TRPV channels. *Sci. Rep.* **2016**, *6*, 27652. [[CrossRef](#)]
65. Thyagarajan, B.; Lukacs, V.; Rohacs, T. Hydrolysis of Phosphatidylinositol 4,5-Bisphosphate Mediates Calcium-induced Inactivation of TRPV6 Channels. *J. Biol. Chem.* **2008**, *283*, 14980–14987. [[CrossRef](#)]
66. Petersen, E.N.; Gudheti, M.; Pavel, M.A.; Murphy, K.R.; Ja, W.W.; Jorgensen, E.M.; Hansen, S.B. Phospholipase D Transduces Force to TREK-1 Channels in a Biological Membrane. *bioRxiv* **2019**. [[CrossRef](#)]

67. Comoglio, Y.; Levitz, J.; Kienzler, M.A.; Lesage, F.; Isacoff, E.Y.; Sandoz, G. Phospholipase D2 specifically regulates TREK potassium channels via direct interaction and local production of phosphatidic acid. *Proc. Natl. Acad. Sci. USA* **2014**, *111*, 13547–13552. [[CrossRef](#)]
68. Cabanos, C.; Wang, M.; Han, X.; Hansen, S.B. A Soluble Fluorescent Binding Assay Reveals PIP₂ Antagonism of TREK-1 Channels. *Cell Rep.* **2017**, *20*, 1287–1294. [[CrossRef](#)]
69. Levitan, I. Cholesterol and Kir channels. *IUBMB Life* **2009**, *61*, 781–790. [[CrossRef](#)]
70. Tikku, S.; Epshtein, Y.; Collins, H.; Travis, A.J.; Rothblat, G.H.; Levitan, I. Relationship between Kir2.1/Kir2.3 activity and their distributions between cholesterol-rich and cholesterol-poor membrane domains. *Am. J. Physiol. Physiol.* **2007**, *293*, C440–C450. [[CrossRef](#)]
71. Zakany, F.; Kovacs, T.; Panyi, G.; Varga, Z. Direct and indirect cholesterol effects on membrane proteins with special focus on potassium channels. *Biochim. Biophys. Acta Mol. Cell Biol. Lipids* **2020**, *1865*, 158706. [[CrossRef](#)]
72. Rosenhouse-Dantsker, A.; Logothetis, D.E.; Levitan, I. Cholesterol Sensitivity of KIR2.1 Is Controlled by a Belt of Residues around the Cytosolic Pore. *Biophys. J.* **2011**, *100*, 381–389. [[CrossRef](#)]
73. Le, N.; Abe, J. Regulation of Kir2.1 Function Under Shear Stress and Cholesterol Loading. *J. Am. Heart Assoc.* **2018**, *7*, e008749. [[CrossRef](#)]
74. Bleecker, J.V.; Cox, P.A.; Foster, R.N.; Litz, J.P.; Blosser, M.C.; Castner, D.G.; Keller, S.L. Thickness Mismatch of Coexisting Liquid Phases in Noncanonical Lipid Bilayers. *J. Phys. Chem. B* **2016**, *120*, 2761–2770. [[CrossRef](#)]
75. Cornell, C.E.; Mileant, A.; Thakkar, N.; Lee, K.K.; Keller, S.L. Direct imaging of liquid domains in membranes by cryo-electron tomography. *Proc. Natl. Acad. Sci. USA* **2020**, *117*, 19713–19719. [[CrossRef](#)]
76. Heberle, F.A.; Doktorova, M.; Scott, H.L.; Skinkle, A.D.; Waxham, M.N.; Levental, I. Direct label-free imaging of nanodomains in biomimetic and biological membranes by cryogenic electron microscopy. *Proc. Natl. Acad. Sci. USA* **2020**, *117*, 19943–19952. [[CrossRef](#)]
77. Martinac, B.; Hamill, O.P. Gramicidin A channels switch between stretch activation and stretch inactivation depending on bilayer thickness. *Proc. Natl. Acad. Sci. USA* **2002**, *99*, 4308–4312. [[CrossRef](#)]
78. Wiggins, P.; Phillips, R. Analytic models for mechanotransduction: Gating a mechanosensitive channel. *Proc. Natl. Acad. Sci. USA* **2004**, *101*, 4071–4076. [[CrossRef](#)]
79. Andersen, O.S.; Koeppe, R.E., II. Bilayer Thickness and Membrane Protein Function: An Energetic Perspective. *Annu. Rev. Biophys. Biomol. Struct.* **2007**, *36*, 107–130. [[CrossRef](#)]
80. Deng, Z.; Maksaev, G.; Schlegel, A.M.; Zhang, J.; Rau, M.; Fitzpatrick, J.A.J.; Haswell, E.S.; Yuan, P. Structural mechanism for gating of a eukaryotic mechanosensitive channel of small conductance. *Nat. Commun.* **2020**, *11*, 3690. [[CrossRef](#)]
81. Perozo, E.; Cortes, D.M.; Sompornpisut, P.; Kloda, A.; Martinac, B. Open channel structure of MscL and the gating mechanism of mechanosensitive channels. *Nature* **2002**, *418*, 942–948. [[CrossRef](#)]
82. Zhang, Y.; Daday, C.; Gu, R.-X.; Cox, C.D.; Martinac, B.; de Groot, B.L.; Walz, T. Visualization of the mechanosensitive ion channel MscS under membrane tension. *Nature* **2021**, *590*, 509–514. [[CrossRef](#)]
83. Katsuta, H.; Sawada, Y.; Sokabe, M. Biophysical Mechanisms of Membrane-Thickness-Dependent MscL Gating: An All-Atom Molecular Dynamics Study. *Langmuir* **2018**, *35*, 7432–7442. [[CrossRef](#)]
84. Yao, Y.; Li, J.; Lin, Y.; Zhou, J.; Zhang, P.; Xu, Y. Structural insights into phospholipase D function. *Prog. Lipid Res.* **2020**, *81*, 101070. [[CrossRef](#)]
85. Bramkamp, M.; Lopez, D. Exploring the Existence of Lipid Rafts in Bacteria. *Microbiol. Mol. Biol. Rev.* **2015**, *79*, 81–100. [[CrossRef](#)]
86. Lorent, J.H.; Levental, I. Structural determinants of protein partitioning into ordered membrane domains and lipid rafts. *Chem. Phys. Lipids* **2015**, *192*, 23–32. [[CrossRef](#)]
87. Hartley, J.M.; Chu, T.-W.; Peterson, E.M.; Zhang, R.; Yang, J.; Harris, J.; Kopeček, J. Super-Resolution Imaging and Quantitative Analysis of Membrane Protein/Lipid Raft Clustering Mediated by Cell-Surface Self-Assembly of Hybrid Nanoconjugates. *Chembiochem* **2015**, *16*, 1725–1729. [[CrossRef](#)]
88. Sengupta, P.; Jovanovic-Talisman, T.; Lippincott-Schwartz, J. Quantifying spatial organization in point-localization superresolution images using pair correlation analysis. *Nat. Protoc.* **2013**, *8*, 345–354. [[CrossRef](#)]
89. Van De Linde, S.; Löschberger, A.; Klein, T.; Heidebreder, M.; Wolter, S.; Heilemann, M.; Sauer, M. Direct stochastic optical reconstruction microscopy with standard fluorescent probes. *Nat. Protoc.* **2011**, *6*, 991–1009. [[CrossRef](#)]
90. Stone, M.B.; A Shelby, S.; Núñez, M.F.; Wissner, K.; Veatch, S.L. Protein sorting by lipid phase-like domains supports emergent signaling function in B lymphocyte plasma membranes. *elife* **2017**, *6*, e19891. [[CrossRef](#)]
91. Nayeibosadri, A.; Petersen, E.N.; Cabanos, C.; Hansen, S.B. A Membrane Thickness Sensor in TREK-1 Channels Transduces Mechanical Force. *SSRN Electron. J.* **2018**. [[CrossRef](#)]
92. Meng, B.; Abdullahi, A.; Ferreira, I.A.T.M.; Goonawardane, N.; Saito, A.; Kimura, I.; Yamasoba, D.; Gerber, P.P.; Fatihi, S.; Rathore, S.; et al. Altered TMPRSS2 usage by SARS-CoV-2 Omicron impacts infectivity and fusogenicity. *Nature* **2022**, *603*, 706–714. [[CrossRef](#)]
93. Espinosa, G.; López-Montero, I.; Monroy, F.; Langevin, D. Shear rheology of lipid monolayers and insights on membrane fluidity. *Proc. Natl. Acad. Sci. USA* **2011**, *108*, 6008–6013. [[CrossRef](#)]
94. Henriques, R.; Griffiths, C.; Rego, E.H.; Mhlanga, M.M. PALM and STORM: Unlocking live-cell super-resolution. *Biopolymers* **2011**, *95*, 322–331. [[CrossRef](#)]

95. Raut, P.; Weller, S.R.; Obeng, B.; Soos, B.L.; West, B.E.; Potts, C.M.; Sangroula, S.; Kinney, M.S.; Burnell, J.E.; King, B.L.; et al. Cetylpyridinium chloride (CPC) reduces zebrafish mortality from influenza infection: Super-resolution microscopy reveals CPC interference with multiple protein interactions with phosphatidylinositol 4,5-bisphosphate in immune function. *Toxicol. Appl. Pharmacol.* **2022**, *440*, 115913. [[CrossRef](#)]
96. Zacharias, D.A.; Violin, J.D.; Newton, A.C.; Tsien, R.Y. Partitioning of Lipid-Modified Monomeric GFPs into Membrane Microdomains of Live Cells. *Science* **2002**, *296*, 913–916. [[CrossRef](#)]
97. Brown, D.; London, E. Structure and Origin of Ordered Lipid Domains in Biological Membranes. *J. Membr. Biol.* **1998**, *164*, 103–114. [[CrossRef](#)]
98. Simons, K.; Vaz, W.L.C. Model systems, lipid rafts, and cell membranes. *Annu. Rev. Biophys. Biomol. Struct.* **2004**, *33*, 269–295. [[CrossRef](#)]
99. Schäfer, L.V.; de Jong, D.H.; Holt, A.; Rzepiela, A.J.; de Vries, A.H.; Poolman, B.; Killian, J.A.; Marrink, S.J. Lipid packing drives the segregation of transmembrane helices into disordered lipid domains in model membranes. *Proc. Natl. Acad. Sci. USA* **2011**, *108*, 1343–1348. [[CrossRef](#)]
100. Smotryś, J.E.; Linder, M.E. Palmitoylation of Intracellular Signaling Proteins: Regulation and Function. *Annu. Rev. Biochem.* **2004**, *73*, 559–587. [[CrossRef](#)] [[PubMed](#)]
101. Salaun, C.; Greaves, J.; Chamberlain, L.H. The intracellular dynamic of protein palmitoylation. *J. Cell Biol.* **2010**, *191*, 1229–1238. [[CrossRef](#)] [[PubMed](#)]
102. Zhang, F.L.; Casey, P.J. PROTEIN PRENYLATION: Molecular Mechanisms and Functional Consequences. *Annu. Rev. Biochem.* **1996**, *65*, 241–269. [[CrossRef](#)]
103. Wang, M.; Casey, P.J. Protein prenylation: Unique fats make their mark on biology. *Nat. Rev. Mol. Cell Biol.* **2016**, *17*, 110–122. [[CrossRef](#)]
104. Chung, H.-W.; Petersen, E.N.; Cabanos, C.; Murphy, K.R.; Pavel, M.A.; Hansen, A.S.; Ja, W.W.; Hansen, S.B. A Molecular Target for an Alcohol Chain-Length Cutoff. *J. Mol. Biol.* **2018**, *431*, 196–209. [[CrossRef](#)]
105. Tanaka, K.A.K.; Suzuki, K.G.N.; Shirai, Y.M.; Shibutani, S.T.; Miyahara, M.S.H.; Tsuboi, H.; Yahara, M.; Yoshimura, A.; Mayor, S.; Fujiwara, T.K.; et al. Membrane molecules mobile even after chemical fixation. *Nat. Methods* **2010**, *7*, 865–866. [[CrossRef](#)]
106. Lang, T.; Bruns, D.; Wenzel, D.; Riedel, D.; Holroyd, P.; Thiele, C.; Jahn, R. SNAREs are concentrated in cholesterol-dependent clusters that define docking and fusion sites for exocytosis. *EMBO J.* **2001**, *20*, 2202–2213. [[CrossRef](#)]
107. DeSpensa, T.; Carlson, M.; Panchagnula, S.; Robert, S.; Duy, P.Q.; Mermin-Bunnell, N.; Reeves, B.C.; Kundishora, A.; Elsamadicy, A.A.; Smith, H.; et al. PTEN mutations in autism spectrum disorder and congenital hydrocephalus: Developmental pleiotropy and therapeutic targets. *Trends Neurosci.* **2021**, *44*, 961–976. [[CrossRef](#)]
108. Pike, L.J.; Han, X.; Chung, K.-N.; Gross, R.W. Lipid Rafts Are Enriched in Arachidonic Acid and Plasmenylethanolamine and Their Composition Is Independent of Caveolin-1 Expression: A Quantitative Electrospray Ionization/Mass Spectrometric Analysis. *Biochemistry* **2002**, *41*, 2075–2088. [[CrossRef](#)]
109. Van Rheenen, J.; Achame, E.M.; Janssen, H.; Calafat, J.; Jalink, K. PIP₂ signaling in lipid domains: A critical re-evaluation. *EMBO J.* **2005**, *24*, 1664–1673. [[CrossRef](#)]

Disclaimer/Publisher’s Note: The statements, opinions and data contained in all publications are solely those of the individual author(s) and contributor(s) and not of MDPI and/or the editor(s). MDPI and/or the editor(s) disclaim responsibility for any injury to people or property resulting from any ideas, methods, instructions or products referred to in the content.